Electronic supplementary information

An ultrasound-assisted approach to bio-derived nanoporous carbons: disclosing a linear relationship between effective micropore and capacitance

Peiyao Bai, Shilin Wei, Xiaoxian Lou and Lang Xu*

MOE Key Laboratory of Coal Processing and Efficient Utilization, School of Chemical Engineering and Technology, China University of Mining and Technology, 1 Daxue Road, Xuzhou, Jiangsu, 221116, China

*Corresponding author. *E-mail address: lang.xu@cumt.edu.cn* (L. Xu)

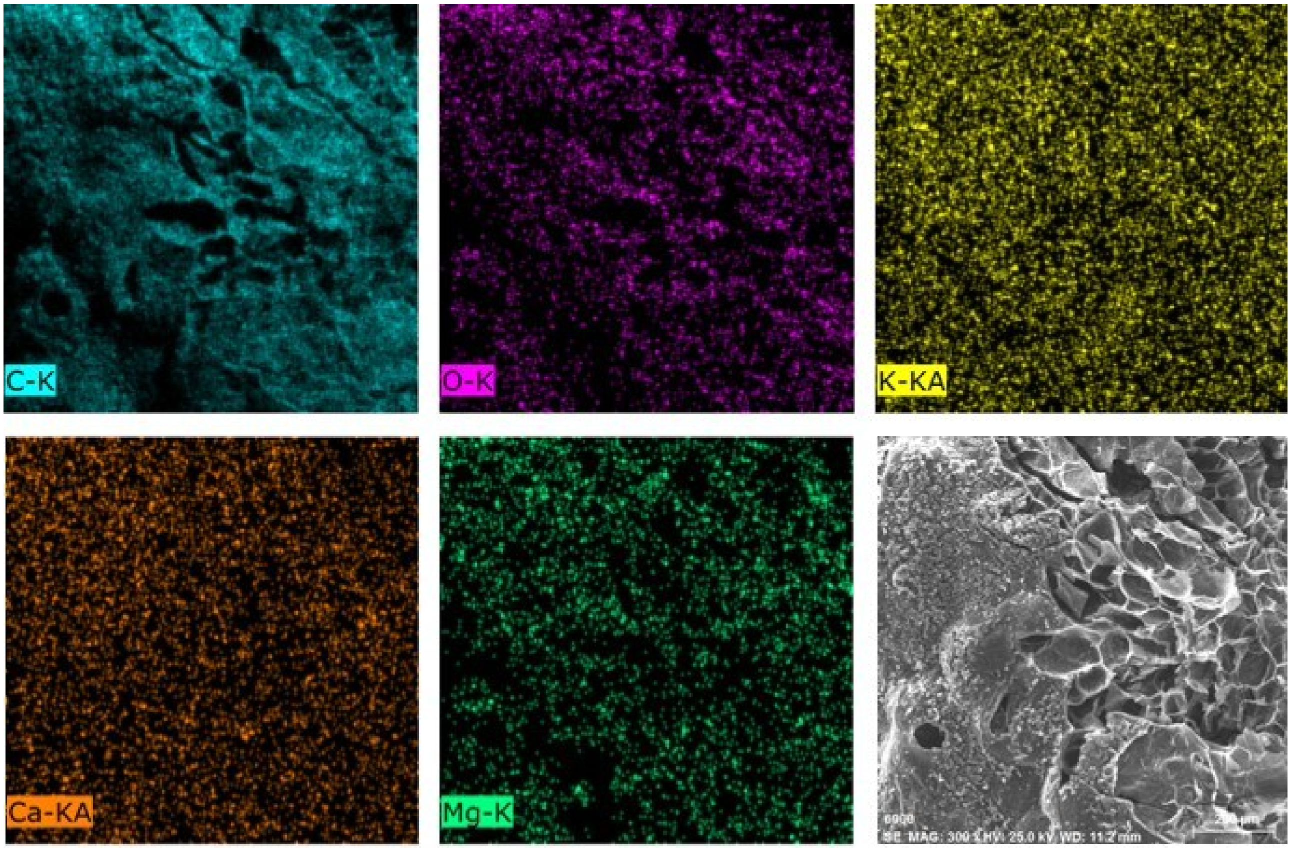

Fig. S1 EDS analyses of the pre-carbonized (400℃) MS.

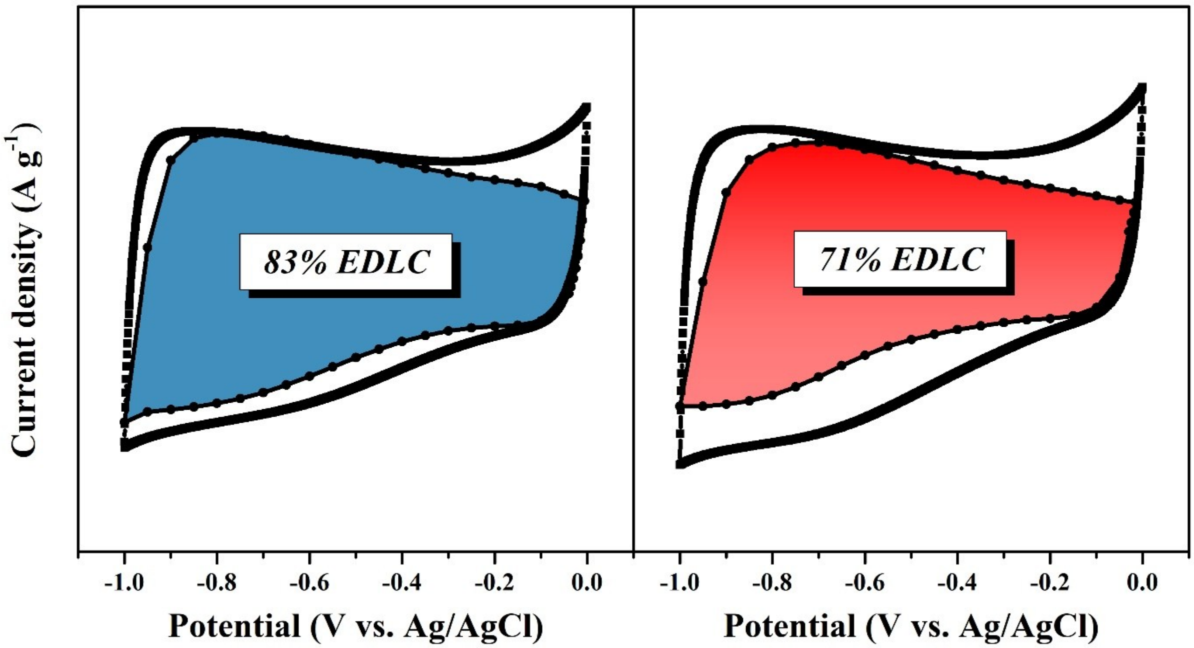

Fig. S2 EDLC contributions depicted in the CV curves of MSPC-850 (left) and MSNPC-850 (right) at a scan rate of 0.02 V s^{-1} in the three-electrode system using 6 M KOH. EDLC contributions are calculated according to Eq. 6 and showed in colour.

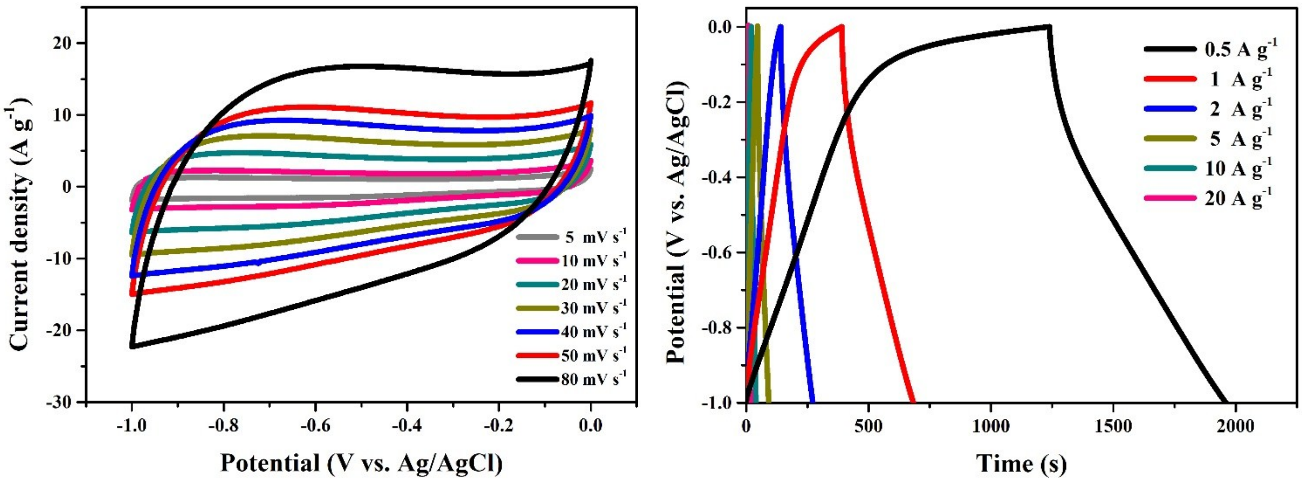

Fig. S3 Electrochemical performances of MSNPC-850* in the three-electrode system using 6 M KOH: (A) CV curves at the different scan rates, (B) GCD curves at the different current densities.

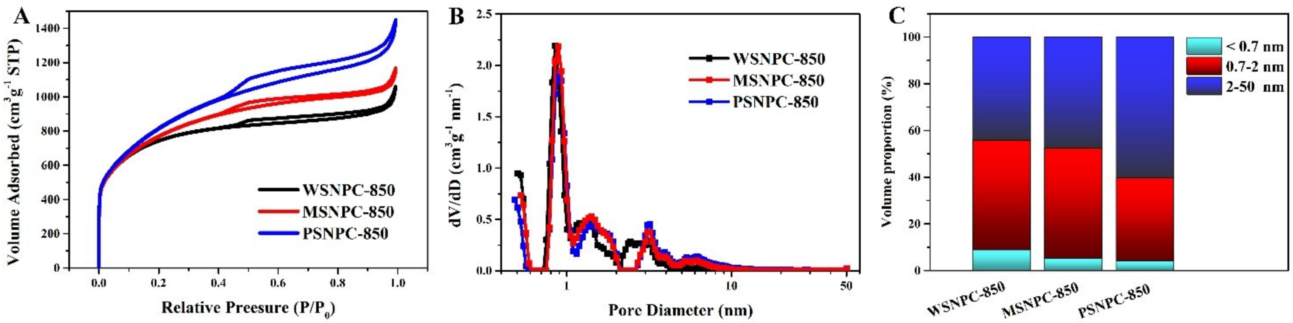

Fig. S4 (A) N_2 adsorption-desorption isotherms, (B) pore size distributions calculated by DFT method, (C) volume-proportion histograms of each pore size segment (<0.7, 0.7-2 and 2-50 nm) of WSNPC-850, MSNPC-850 and PSNPC-850.

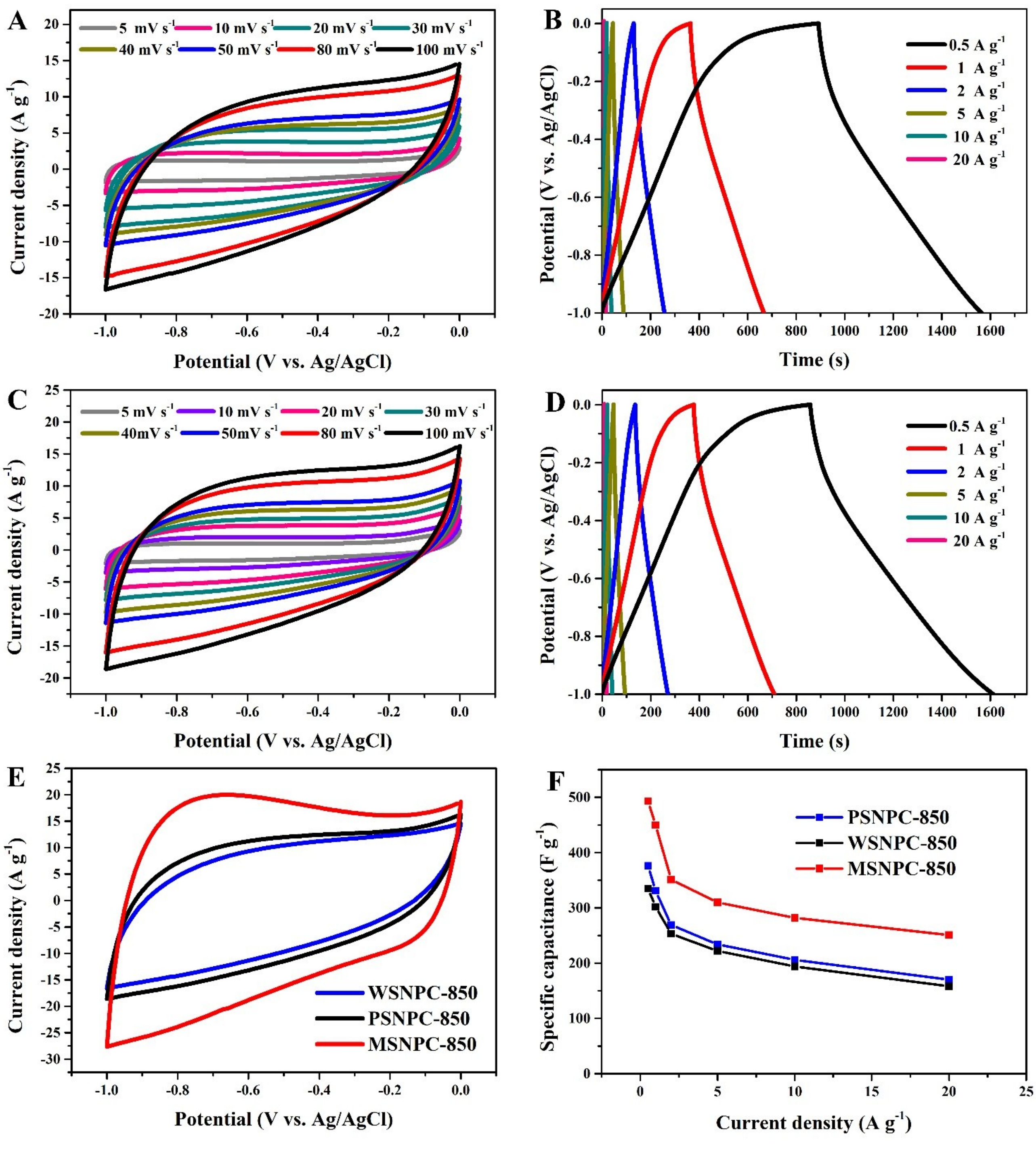

Fig. S5 Electrochemical performances in the three-electrode system using 6 M KOH: CV curves of (A) WSNPC-850 and (C) PSNPC-850 at the different scan rates; GCD curves of (B) WSNPC-850 and (D) PSNPC-850 at the different current densities; (E) CV curves of WSNPC-850, PSNPC-850 and MSNPC-850 at 100 mV s^{-1}; (F) rate performance of WSNPC-850, PSNPC-850 and MSNPC-850.

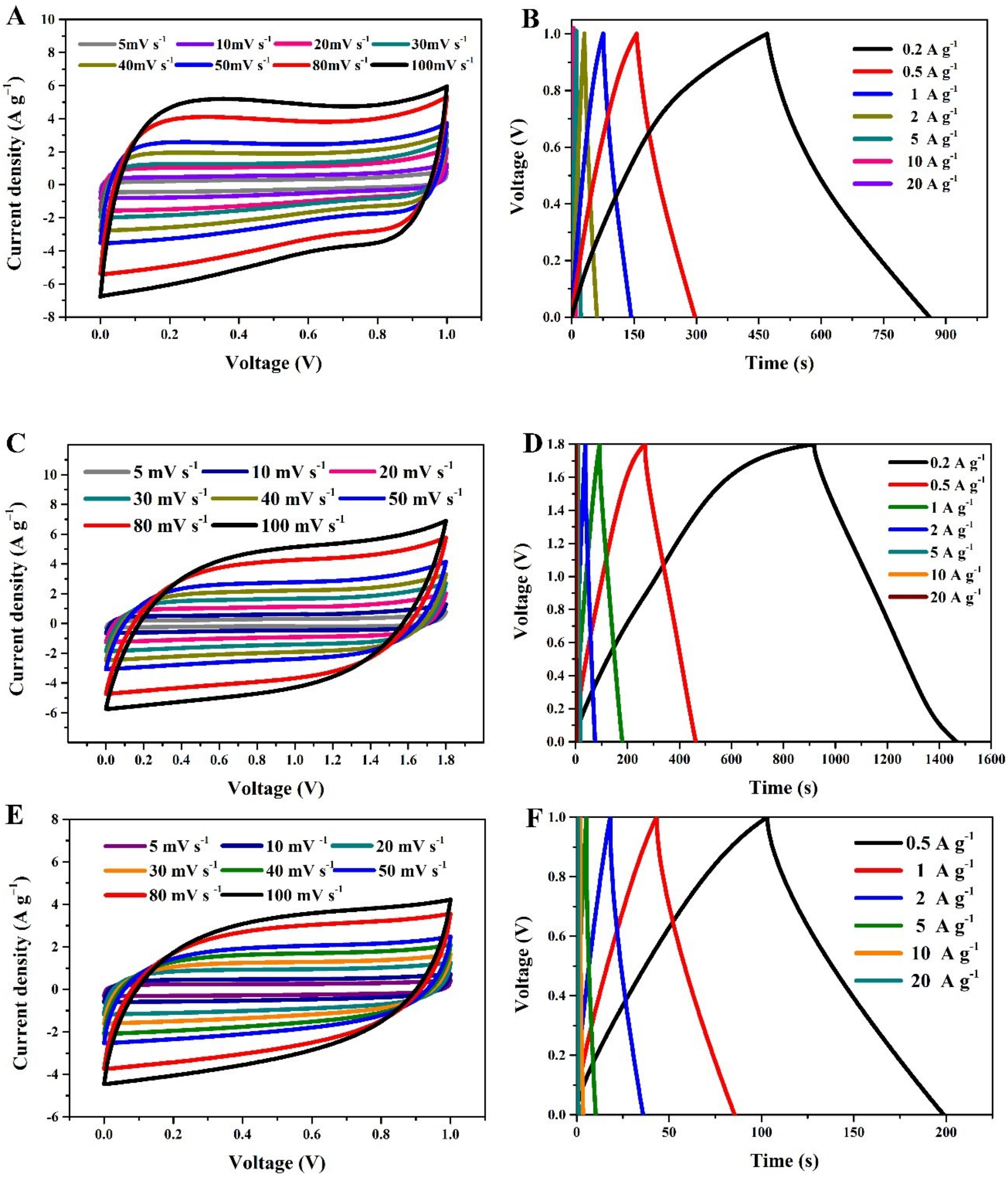

Fig. S6 Electrochemical performance of the supercapacitor MSNPC-850//MSNPC-850 in the different electrolytes: CV curves at the different scan rates in (A) 6 M KOH, (C) 1 M Na_2SO_4 and (E) 6 M NaOH; GCD curves at the different current densities in (B) 6 M KOH, (D) 1 M Na_2SO_4 and (F) 6 M NaOH. MSNPCs, PSNPC-850 and WSNPC-850 in 6 M KOH at the different current densities.

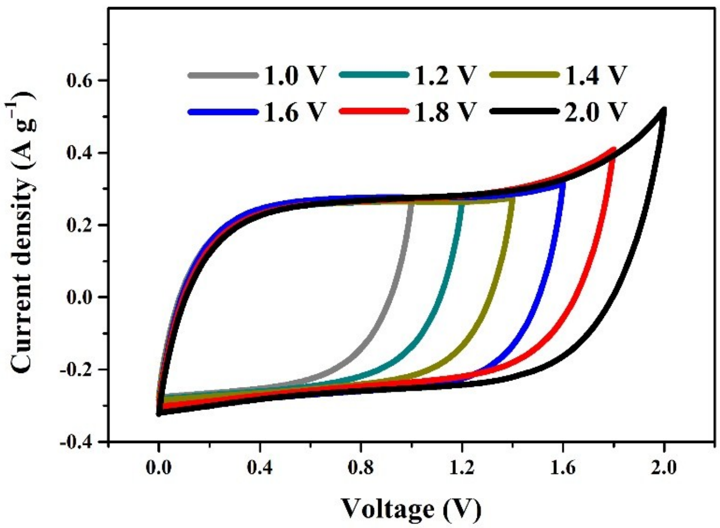

Fig. S7 CV curves with the different voltage windows (1.0-2.0 V) in 1 M Na_2SO_4.

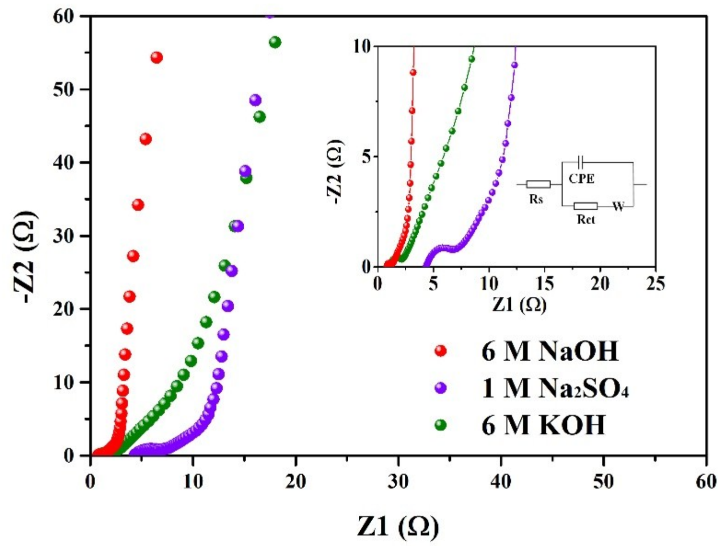

Fig. S8 Nyquist plots of MSNPC-850//MSNPC-850 in the different electrolytes: 6 M NaOH, 1 M Na_2SO_4 and 6 M KOH.

Table S1 Comparison of specific capacitance of supercapacitor materials derived from different carbon precursors in the three-electrode system

Specific capacitance / F g^{-1}	Current density / A g^{-1}	Electrolyte	Carbon precursor	Ref
222	0.5	6 M KOH	Bamboo	S1
273.8	1	1 M KOH	konjac	S2
312	1	1 M H_2SO_4	gelatin and citric acid	S3
289	0.5	6 M KOH	jujun grass	S4
353	1	6 M KOH	algae microsphere	S5
339	0.5	1 M H_2SO_4	cellulose carbamate	S6
289	0.5	2 M KOH	wood scraps	S7
420	0.5	6 M KOH	styrene acrylonitrile	S8
240	0.5	2 M KOH	coconut shell and sewage sludge	S9
213	0.1	6 M KOH	root of Multibract Raspberry	S10
212	0.5	6 M KOH	carbon nanoflakes	S11
190	1	1 M $TEABF_4$/AN	cattle bone	S12
493	0.5	6 M KOH	mango skin	This work

Table S2 Specific capacitances of MSNPCs, WSNPC-850 and PSNPC-850 in the three-electrode system using 6 M KOH

Sample	Specific capacitance / F g^{-1}					
Current density / A g^{-1}	0.5	1	2	5	10	20
MSNPC-750	126	110	100	91	85	76
MSNPC-850	493	450	351	310	282	251
MSNPC-950	260	206	167	152	143	136
WSNPC-850	335	302	253	222	194	158
PSNPC-850	376	331	269	234	206	170

Table S3 Equivalent circuit fit results of MSNPCs [a]

Sample	R_s / Ω	R_{ct} / Ω	W / Ω	Q
MSNPC-750	0.970	1.017	0.064	1.15×10^{-4}
MSNPC-850	0.776	0.335	0.214	2.34×10^{-4}
MSNPC-950	0.720	0.220	0.495	8.40×10^{-4}

[a] R_s represents the combined series resistance; R_{ct} represents the charge-transfer resistance; W represents the Warburg diffusion resistance; Q represents the constant phase element.

Table S4 Equivalent circuit fit results of MSNPC-850//MSNPC-850 in the different electrolytes [a]

Electrolyte	R_s / Ω	R_{ct} / Ω	W / Ω	Q
6 M KOH	0.776	0.335	0.214	2.34×10^{-4}
6 M NaOH	1.138	0.918	0.090	2.38×10^{-4}
1 M Na_2SO_4	4.340	2.646	0.103	1.50×10^{-4}

[a] R_s represents the combined series resistance; R_{ct} represents the charge-transfer resistance; W represents the Warburg diffusion resistance; Q represents the constant phase element.

References

(S1) Y. Gong, D. Li, C. Luo, Q. Fu and C. Pan, *Green Chem.*, 2017, **19**, 4132-4140.

(S2) Q. Li, X. Bai, Q. Meng, T. Chen, W. Zhu, W. Yao, J. Lei, L. Zhang, X. Yang, X. Wei and T. Duan, *Appl. Surf. Sci.*, 2018, **448**, 16-22.

(S3) Y. Shi, L. Zhang, T. B. Schon, H. Li, C. Fan, X. Li, H. Wang, X. Wu, H. Xie and H. Sun, *ACS Appl. Mater. Interfaces*, 2017, **9**, 42699-42707.

(S4) Y. Liu, B. Huang, X. Lin and Z. Xie, *J. Mater. Chem. A*, 2017, **5**, 13009-13018.

(S5) B. Zhu, B. Liu, C. Qu, H. Zhang, W. Guo, Z. Liang, F. Chen and R. Zou, *J. Mater. Chem. A*, 2018, **6**, 1523-1530.

(S6) X. Zhou, P. Wang, Y. Zhang, L. Wang, L. Zhang, L. Zhang, L. Xu and L. Liu, *J. Mater. Chem. A*, 2017, **5**, 12958-12968.

(S7) S. Zhang, C. Wu, W. Wu, C. Zhou, Z. Xi, Y. Deng, X. Wang, P. Quan, X. Li and Y. Luo, *J. Power Sources*, 2019, **424**, 1-7.

(S8) U. Kumar, V. Gaikwad, M. Mayyas, V. Sahajwalla and R. K. Joshi, *J. Power Sources*, 2018, **394**, 140-147.

(S9) L. Peng, Y. Liang, H. Dong, H. Hu, X. Zhao, Y. Cai, Y. Xiao, Y. Liu and M. Zheng, *J. Power Sources*, 2018, **377**, 151-160.

(S10) Y. Yao, Q. Zhang, P. Liu, L. Yu, L. Huang, S. Zeng, L. Liu, X. Zeng and J. Zou, *RSC Adv.*, 2018, **8**, 1857-1865.

(S11) Y. Zhang, Q. Sun, K. Xia, B. Han, C. Zhou, Q. Gao, H. Wang, S. Pu and J. Wu, *ACS Sustainable Chem. Eng.*, 2019, **7**, 5717-5726.

(S12) N. Sun, Z. Li, X. Zhang, W. Qin, C. Zhao, H. Zhang, D. H. L. Ng, S. Kang, H. Zhao and G. Wang, *ACS Sustainable Chem. Eng.*, 2019, **7**, 8735-8743.